

Provided for non-commercial research and education use.  
Not for reproduction, distribution or commercial use.



This article appeared in a journal published by Elsevier. The attached copy is furnished to the author for internal non-commercial research and education use, including for instruction at the authors institution and sharing with colleagues.

Other uses, including reproduction and distribution, or selling or licensing copies, or posting to personal, institutional or third party websites are prohibited.

In most cases authors are permitted to post their version of the article (e.g. in Word or Tex form) to their personal website or institutional repository. Authors requiring further information regarding Elsevier's archiving and manuscript policies are encouraged to visit:

<http://www.elsevier.com/authorsrights>



ELSEVIER



CrossMark

Available online at [www.sciencedirect.com](http://www.sciencedirect.com)

ScienceDirect

Journal of the European Ceramic Society 34 (2014) 373–379

[www.elsevier.com/locate/jeurceramsoc](http://www.elsevier.com/locate/jeurceramsoc)

# Fabrication of apatite-type lanthanum silicate films and anode supported solid oxide fuel cells using nano-sized printable paste

Hideki Yoshioka<sup>a,\*</sup>, Hiroyuki Mieda<sup>b</sup>, Takahiro Funahashi<sup>b</sup>, Atsushi Mineshige<sup>b</sup>, Tetsuo Yazawa<sup>b</sup>, Ryohei Mori<sup>c</sup>

<sup>a</sup> Hyogo Prefectural Institute of Technology, Suma-ku, Kobe, Hyogo 654-0037, Japan

<sup>b</sup> Department of Materials Science and Chemistry, Graduate School of Engineering, University of Hyogo, Himeji, Hyogo 671-2201, Japan

<sup>c</sup> Fuji-Pigment Co. Ltd., Kawanishi, Hyogo 666-0015, Japan

Received 14 May 2013; received in revised form 29 August 2013; accepted 30 August 2013

Available online 24 September 2013

## Abstract

Apatite-type lanthanum silicate based films have attracted significant interests to use as an electrolyte of solid oxide fuel cells (SOFCs) working at intermediate temperature. We have prepared Mg doped lanthanum silicate (MDLS) films on NiO–MDLS cermet substrates by spin coating and sintering of nano-sized printable paste made by beads milling. Changes in crystal structure and microstructure of the paste films with the sintering temperature have been investigated to show that porous network structure with a grain growth evolves up to 1300 °C, whereas densification occurred above 1400 °C. Anode supported SOFCs using the pasted MDLS films were successfully fabricated: an open circuit voltage of 0.91 V and a maximum power density of 150 mW cm<sup>-2</sup> measured at 800 °C were obtained with the electrolyte film sintered at 1500 °C.

© 2013 Elsevier Ltd. All rights reserved.

**Keywords:** Apatite-type ionic conductor; Lanthanum silicate; Solid oxide fuel cell; Nano-sized paste; Anode support

## 1. Introduction

Solid oxide fuel cells (SOFCs) have attracted great interest as clean and high efficient electrical power sources. Reduction of operating temperature of SOFCs down to intermediate temperature (500–700 °C) gives significant advantages such as wider ranges of material selection, longer life and lower manufacturing costs.<sup>1,2</sup> Development of solid electrolytes which exhibit high ionic conductivity at reduced temperature is one of the key issues for the commercialization of intermediate temperature solid oxide fuel cells (IT-SOFCs). However, ionic conductivity of a common SOFC solid electrolyte, yttria stabilized zirconia (YSZ) rapidly reduces as temperature decreases. Numbers of research have been done searching for solid electrolyte materials which exhibit high ionic conductivity even at intermediate temperature range such as doped ceria<sup>3</sup> and doped lanthanum gallate<sup>4</sup> type solid electrolyte materials.

Nakayama et al. have first demonstrated that apatite-type lanthanum silicate exhibits high ionic conductivity and high oxide-ion transport number even at intermediate temperature range.<sup>5</sup> Ionic conductivity of the lanthanum silicate was found to be enhanced by introduction of excess oxide ions<sup>6</sup> and cation doping into La or Si sites.<sup>7,8</sup> Among them, Al doping into the Si site of oxide-ion excess lanthanum silicate gives an marked increase: these apatites showed ionic conductivity of 17–30 mS cm<sup>-1</sup> at 700 °C<sup>9–11</sup> which were higher than YSZ. We have reported that ionic conductivity of lanthanum silicate can be also enhanced by doping Mg into the Si site<sup>12</sup> and has been attempted to be utilized for a solid electrolyte of IT-SOFCs.<sup>13</sup> Mg doped lanthanum silicate (MDLS) exhibits high ionic conductivity comparable to Sr and Mg doped lanthanum gallate at temperatures less than 550 °C.<sup>14</sup> SOFCs using doped lanthanum silicate ceramic electrolytes have shown moderate power densities of 125–250 mW cm<sup>-1</sup> at 800 °C.<sup>14–16</sup> However, fabrication of lanthanum silicate ceramics based SOFC for practical use is still difficult because of the high sintering temperature of lanthanum silicate ceramics (>1600 °C), which prevent us from preparing dense electrolyte films with low manufacturing costs. To overcome this obstacle,

\* Corresponding author at: 3-1-12, Yukihiro-cho, Suma-ku, Kobe, Hyogo 654-0037, Japan. Tel.: +81 78 731 4302; fax: +81 78 735 7845.

E-mail address: [hide@hyogo-kg.jp](mailto:hide@hyogo-kg.jp) (H. Yoshioka).

we have started the research to prepare thin films of lanthanum silicates directly on the electrode substrates as electrode supported-type SOFCs. There are some previous researches to make lanthanum silicate films by sol–gel method,<sup>17</sup> thermal spraying,<sup>18–20</sup> sputtering<sup>21,22</sup> and tape casting.<sup>23</sup> To the best of our knowledge, none of these researches, however, have succeeded in making highly conductive lanthanum silicate films and in preparing electrode supported SOFCs. There is only one paper published by our group reporting the fabrication of anode supported SOFCs using thermal sprayed MDLS films on NiO–MDLS cermet anodes.<sup>24</sup> We have shown in this paper that the thermal sprayed MDLS films could be crystallized above 800 °C to be an oxide-ion conductor. The SOFC thus obtained showed a maximum power density of 80 mW cm<sup>-2</sup> at 800 °C with a common (La<sub>0.6</sub>Sr<sub>0.4</sub>)(Co<sub>0.8</sub>Fe<sub>0.2</sub>)O<sub>3-δ</sub> (LSCF) cathode material.

The purpose of this study is to develop a more versatile and cost-effective procedure to make SOFCs having high power densities at intermediate temperature by using highly conductive MDLS electrolyte films. We have successfully fabricated dense electrolyte films from printable paste consisting of nano-sized MDLS particles made by bead milling technique. This paper reports fabrication of dense MDLS electrolyte films by spin coating of the paste and application to anode supported SOFCs. Optimization of the cell structure and the fabrication procedure including electrode microstructure control to increase power density is under investigation and the results will be published elsewhere.

## 2. Experimental

### 2.1. Preparation of nano-sized MDLS paste

MDLS powder with a composition of La<sub>9.8</sub>Si<sub>5.7</sub>Mg<sub>0.3</sub>O<sub>26.4</sub> was prepared by a conventional solid state reaction of La<sub>2</sub>O<sub>3</sub>, SiO<sub>2</sub> and MgO powders at 1600 °C, followed by grinding and sieving according to the particle sizes. Powders with particle sizes less than 10 μm are used for fabrication of both MDLS paste and anode substrates.

MDLS printable paste for spin coating was prepared by mixing the powder and polyoxyethylene sorbitan tristearate as a dispersant (Kao Corporation, Japan) in terpineol (Arakawa Chemical Industries Co. Ltd., Japan) with zircon beads using a stirring machine rotating for 30 min at 3500 rpm. The viscous paste was made by combining 21 g of MDLS powder with 2 g of dispersant and 47 g of terpineol. Then 3 g of ethyl cellulose (Nisshin Kasei Co. Ltd., Japan, *M<sub>w</sub>* 20,000) was added to 45 g of sol slurry as a binder to increase viscosity and stirred for an additional 30 min at 2000 rpm to completely dissolve ethyl cellulose.

Thermogravimetry (TG) and differential thermal analysis (DTA) were performed using a TG-DTA system (Thermoplus EVO TG-8120, RIGAKU Corp., Japan) to evaluate the thermal properties of the MDLS paste. Air flow rate and temperature scanning rate were set to 300 ml min<sup>-1</sup> and 20 °C min<sup>-1</sup>, respectively.

### 2.2. Preparation and characterization of MDLS paste films

NiO and MDLS powders were mixed in 6:4 in weight ratio and pressed into disks of 13 mm in diameter and 1.5 mm in thickness. They were sintered at 1400 °C for 4 h to obtain cermet anode substrates. MDLS pastes were spin-coated on the cermet anode substrates with a spinning rate of 5000 rpm for 30 s. They were dried at 180 °C for 10 min and then heated at 500 °C for 10 min to burn out organic component. After repeating this procedure for 4 times, the MDLS films on the anode substrates were finally sintered for 4 h at various temperatures between 1000 and 1500 °C.

Phases in the films were investigated by X-ray diffraction (XRD) method using a powder diffractometer (RAD-RU, Rigaku Corp.) with Cu Kα radiation of 40 kV–200 mA. Film structures were examined by a field-emission type scanning electron microscope (SEM) (Sirion, FEI company) with an acceleration voltage of 5 or 10 kV.

### 2.3. Fabrication and evaluation of anode supported SOFCs

Anode supported single cells were obtained by screen-printing La<sub>0.6</sub>Sr<sub>0.4</sub>Co<sub>0.2</sub>Fe<sub>0.8</sub>O<sub>3</sub> (LSCF) cathode paste to the electrolyte film surfaces and heated at 1000 °C. The cathode paste was prepared by mixing LSCF powder in terpineol solvent. Then, Pt paste electrodes of 8 mm in diameter were painted on both LSCF and anode substrate faces and fired again at 1000 °C to ensure the electrical contact. This single cell was applied to SOFC evaluation equipment and heated to 1000 °C to complete glass ceiling and set down to 800 °C. Thus, oxygen was supplied to cathode side and H<sub>2</sub>–Ar gas was supplied to anode side to reduce NiO in the anode substrates. After open circuit voltages (OCV) became stable, current–voltage (*I*–*V*) characteristic curves were measured using a galvanostat and an electrometer, which then gave current–power densities (*I*–*P*) characteristic curves. AC impedances at an open circuit state were measured by a BAS ALS-760C impedance analyzer with frequencies ranging from 100 kHz to 10 mHz. *I*–*V* characteristic curves and AC impedance measurements were performed at 800, 700 and then 600 °C.

## 3. Results and discussion

### 3.1. Preparation of MDLS paste films

Fig. 1 shows TG–DTA curves of the MDLS paste. The TG curve revealed that approximately a half of organic solvent, terpineol, was evaporated until 250 °C followed by a gradual decomposition of dispersing chemical and resin observed up to 450 °C. Exothermic DTA peaks of 401 °C and 422 °C are ascribed to decompositions of ethyl cellulose and dispersing chemical, respectively. Thus, complete decomposition of dispersing chemical and resin would be expected when 500 °C was applied after spin coating.

Fig. 2 shows pictures of (a) an anode substrate and (b) a film surface after spin coating and heating at 500 °C for 4 times. Fig. 2(c)–(h) are film surfaces after heated at 1000–1500 °C.

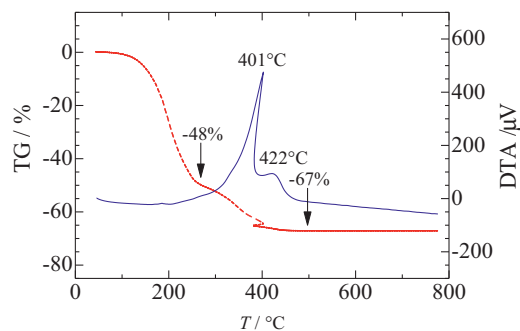


Fig. 1. TG-DTA curves of MDLS paste.

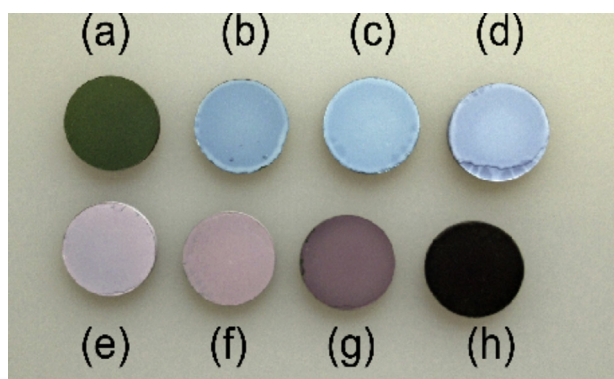


Fig. 2. Photos of (a) an anode substrate, (b) MDLS paste spin-coated 4 times on an anode substrate, films sintered at (c) 1000°C, (d) 1100°C, (e) 1200°C, (f) 1300°C, (g) 1400°C and (h) 1500°C.

A surface of (a) an anode substrate is deep green due to NiO included in the cermet. Film surfaces of (b)–(d) are white due to light scattering by fine particles in the pasted film. Film surfaces of (e)–(g) show a change in color from white to reddish brown. This indicates that sintering and grain growth of the MDLS paste proceeds gradually between 1200°C and 1400°C. Then a dense transparent film with a smooth surface roughness is finally obtained at 1500°C (h).

SEM images of the film surfaces after heating at 1000–1500°C are shown in Fig. 3(a)–(f). Fig. 3(a) shows that the film heated at 1000°C has a small grain size (50–300 nm) of MDLS particles which seems to be same as the particle size in the paste. Grain growths of the nano-sized particles were observed with formation of network above 1100°C. Below 1300°C, however, the films still include a lot of pores, showing porous network structure. Both the grain sizes and pore sizes increased simultaneously as the temperature increased from 1100 to 1200 and 1300°C. Contrarily, above 1400°C, pores are decreasing rapidly until fully dense surface structure, observed in the sample heated at 1500°C. Microstructures of (e) and (f) reveals a melt sintering process occurred in the pasted films above 1400°C.

Fig. 4(a)–(f) are corresponding fractured cross sections of the films. In agreement with the surface SEM images, porous network structure is gradually formed with grain growth of each particle below 1300°C, followed by densification of the film occurred above 1400°C, resulting in the very dense microstructures of Fig. 4(f). In harmony with the densification, film thickness of 20 μm observed in Fig. 4(a) decreased to 15 μm in Fig. 4(f) after heated at 1500°C.

The above microstructure observation reveals that the sintering and densification of nano-sized particles in the MDLS paste proceed above 1400°C, which is 200°C lower than the conventional solid state reaction. Lowering of the sintering temperature is beneficial for preparing anode supported SOFCs which require dense electrolyte layers on porous anode materials such as NiO based cermets. The anode materials in general cannot be heated at high temperatures to maintain porosity and avoid unwanted reaction.

Fig. 5(a) shows X-ray diffraction (XRD) patterns of (i) the anode substrate, (ii) the spin-coated film and the films sintered at (iii) 1000°C, (iv) 1100°C, (v) 1200°C, (vi) 1300°C, (vii) 1400°C and (viii) 1500°C. XRD peaks of the anode substrate are attributed to NiO and apatite-type phases, indicating that no side reaction occurred during the anode fabrication process at 1400°C. As for the paste films, only an apatite-type phase was observed in all films up to 1500°C. A close observation,

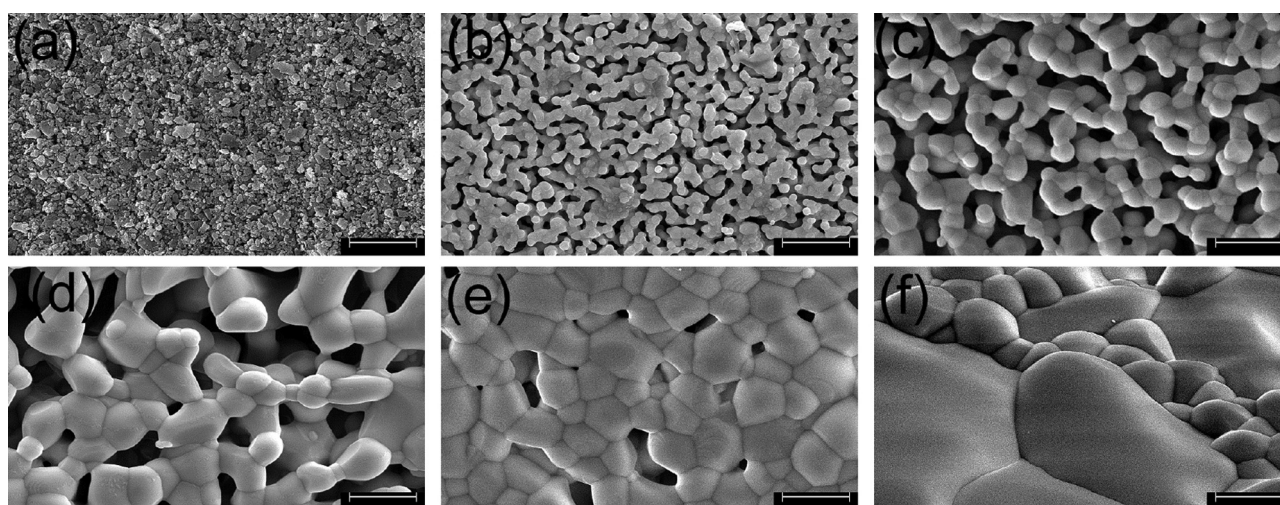


Fig. 3. SEM images of the film surfaces sintered for 4 h at (a) 1000°C, (b) 1100°C, (c) 1200°C, (d) 1300°C, (e) 1400°C and (f) 1500°C. Micron bars show 2 μm.

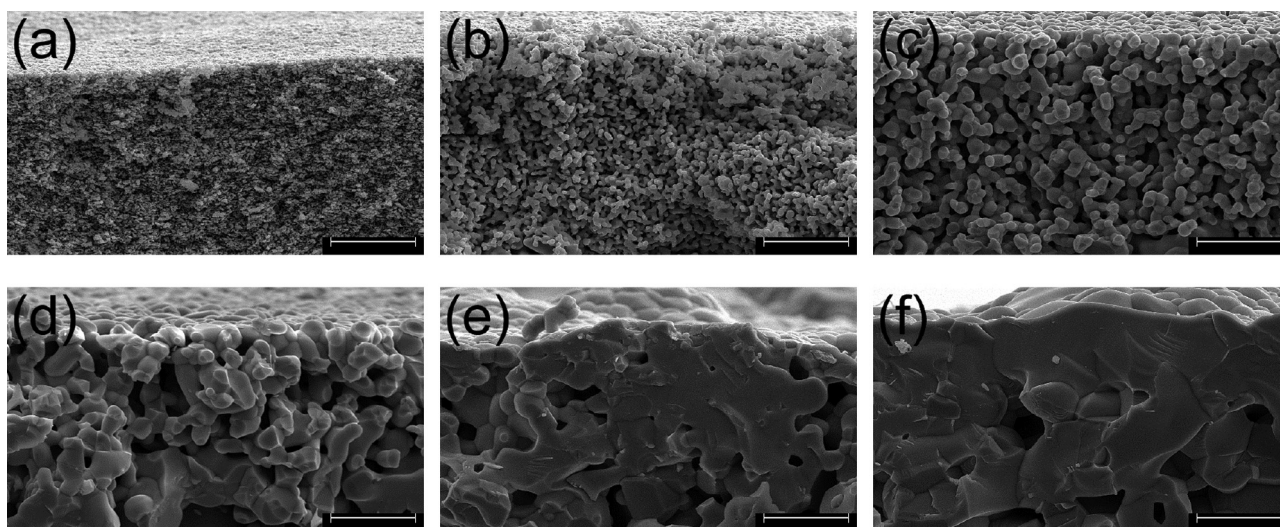


Fig. 4. SEM images of the fractured surfaces of the films sintered for 4 h at (a) 1000 °C, (b) 1100 °C, (c) 1200 °C, (d) 1300 °C, (e) 1400 °C and (f) 1500 °C. Micron bars show 5 μm.

however, reveals a change in the peak widths, the peak positions and the relative intensities with the sintering temperature. Broad peaks of (ii) the spin-coated paste gradually change to sharp peaks observed in the films heated at high temperatures because of grain growth and release of stress which has been introduced in the milling process. In addition, relative intensities of the particular XRD peaks such as 002 and 004 apparently increase with increasing sintering temperature compared with other peaks. This suggests a preference of orientation along c-axis in the MDLS apatite phase with densification.

Fig. 5(b) displays XRD patterns ( $2\theta = 25\text{--}35^\circ$ ) of the anode substrate and the films which demonstrate a change in peak shapes and positions of the 211, 112 and 300 peaks. Obviously, peak positions of the films heated at 500–1300 °C shift to the higher angle side compared with a MDLS phase in the anode substrate. This implies lattice shrinkage due to compressive stress induced in the paste milling process. On the other hand, in the films heated at 1400 and 1500 °C, 211 and 300 peaks restore the positions of the anode substrate revealing a release of the stress during the densification process. Additionally, a clear

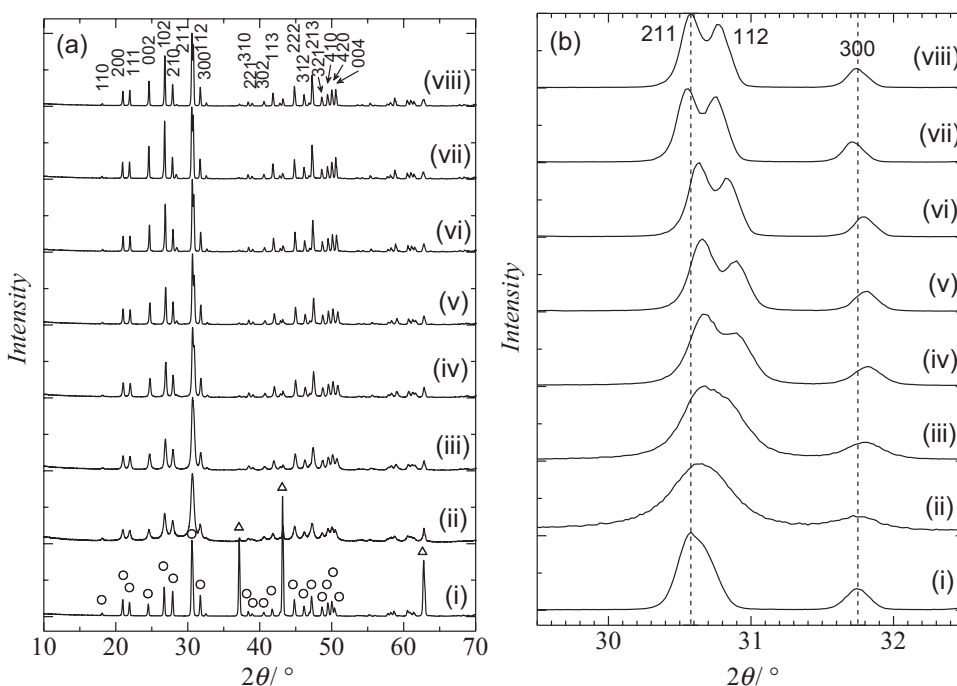


Fig. 5. (a) XRD patterns of (i) the anode substrate, the spin-coated films heated for 4 h at (ii) 500 °C, (iii) 1000 °C, (iv) 1100 °C, (v) 1200 °C, (vi) 1300 °C, (vii) 1400 °C and (viii) 1500 °C. Anode substrate consists of NiO (open triangle) and apatite phase (open circle). (b) Enlarged figure shows 211, 112 and 300 peaks.

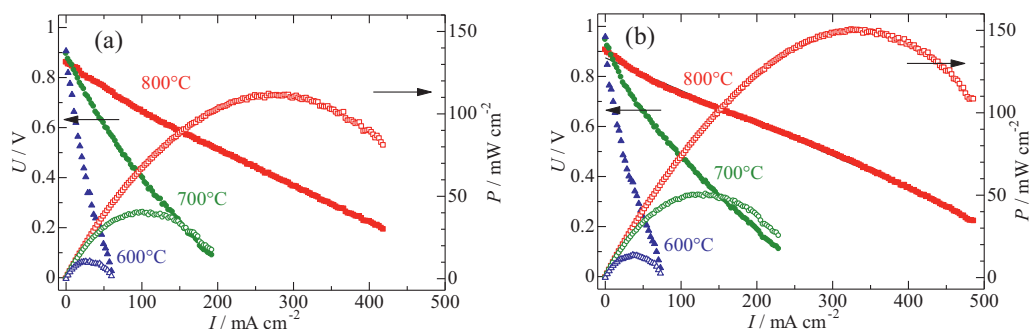


Fig. 6.  $I$ - $V$  and  $I$ - $P$  characteristic curves of the SOFC-A and B at 800, 700 and 600 °C.

separation of 2 1 1 and 1 1 2 peaks is found to be characteristic of the pasted films heated above 1000 °C. At present, however, a relationship between the film microstructures and transport properties was not clear and remains to be further studied in order to prepare high performance pasted electrolyte films.

### 3.2. Electrochemical properties of the anode supported SOFC

Electrochemical properties were investigated on two SOFCs having pasted MDLS electrolyte films which were spin-coated on NiO–MDLS cermet disks and sintered for 4 h at 1400 °C and 1500 °C. Materials and fabrication conditions are listed in Table 1. Screen-printed LSCF pastes fired at 1000 °C were used as a cathode.  $I$ - $V$  and  $I$ - $P$  characteristic curves of the SOFC-A and B at 800, 700 and 600 °C are shown in Fig. 6(a) and (b), respectively. Open circuit voltages (OCVs) of the SOFC-A were 0.86–0.91 V, which were significantly lower than the theoretical value (1.1 V). Since SOFCs using sintered ceramic electrolytes of MDLS showed OCVs being equal to the theoretical value,<sup>13,14</sup> lower OCVs observed for SOFC-A are ascribed to a gas leak through pores and cracks in the thin electrolyte film. The SOFC-B showed slightly higher OCVs of 0.91–0.96 V due to a denser electrolyte film. The OCVs, however, are still low compared to the theoretical value. Thus, there must be a small gas leak through the electrolyte film of the SOFC-B.

Maximum power densities of the SOFC-A were 112, 40 and 11 mW cm<sup>-2</sup> at 800, 700 and 600 °C, respectively. Densification of the electrolyte film brought about an enhancement on power densities of the SOFC-B as 150, 51 and 14 mW cm<sup>-2</sup> at 800, 700 and 600 °C, respectively. AC impedances at 800, 700 and 600 °C measured for the SOFC-A and B are shown in Fig. 7. Ohmic resistances and polarization resistances are listed in Table 2 along with the OCVs and the maximum power

densities. The AC impedance results evidently show that higher power densities at 800 and 700 °C of the SOFC-B are ascribed to lower ohmic resistance, while the higher power density at 600 °C is due to both lower ohmic resistance and polarization resistance.

Fig. 8 shows SEM images of the fractured cross sections of the SOFC-A and B after the fuel cell tests. Thickness of the films was 20 and 15 μm for SOFC-A and B, respectively. The porous cermet anode has two types of grains, MDLS particles with 5–10 μm diameter and aggregates of very small Ni particles, with a triple phase boundary spreading into the anode. The porous cathode consists of LSCF particles with a diameter about 1 μm. An electrolyte film of the SOFC-A is fairly dense but includes significant pores and cracks inside. The SOFC-B has a much denser microstructure which can explain higher power densities, OCVs and lower ohmic resistances. Some pores and cracks, however, would be found in the pasted film of the SOFC-B considering the measured OCVs (0.91–0.96 V) although no pores and cracks can be seen in this view of the SEM image.

There are few papers reporting electrochemical properties of anode supported fuel cells based on apatite-type lanthanum silicate electrolyte films. We have reported fuel cell properties of the SOFC having a plasma sprayed electrolyte film with 100 μm thickness and LSCF cathode which showed OCVs of 0.90–0.97 V and maximum power densities of 80, 45 and

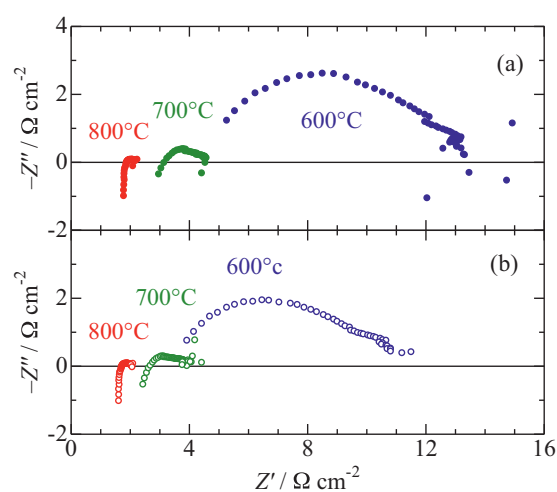


Fig. 7. AC impedance plots of (a) SOFC-A and (b) SOFC-B at 800, 700 and 600 °C.

Table 1  
Materials and fabrication conditions of SOFC-A and B.

Component	Procedure
Anode substrate	NiO–MDLS cermet pressed and heated at 1400 °C
Electrolyte film	MDLS spin-coated and heated at 1400 °C (A) or 1500 °C (B)
Cathode layer	LSCF screen-printed and heated at 1000 °C

Table 2  
Fuel cell properties and area specific resistances of the SOFCs prepared.

Sample	Max. power density ( $\text{mW cm}^{-2}$ )			OCV (V)			Ohmic resistance ( $\Omega \text{ cm}^2$ )			Polarization resistance ( $\Omega \text{ cm}^2$ )		
	800 °C	700 °C	600 °C	800 °C	700 °C	600 °C	800 °C	700 °C	600 °C	800 °C	700 °C	600 °C
A	112	40	11	0.86	0.90	0.91	1.9	3.2	4.6	0.3	1.4	9.6
B	150	51	14	0.91	0.95	0.96	1.7	2.7	3.5	0.4	1.3	7.3
RE	146	78	41	0.87	0.90	0.93	1.8	2.6	3.8	0.1	0.5	1.8

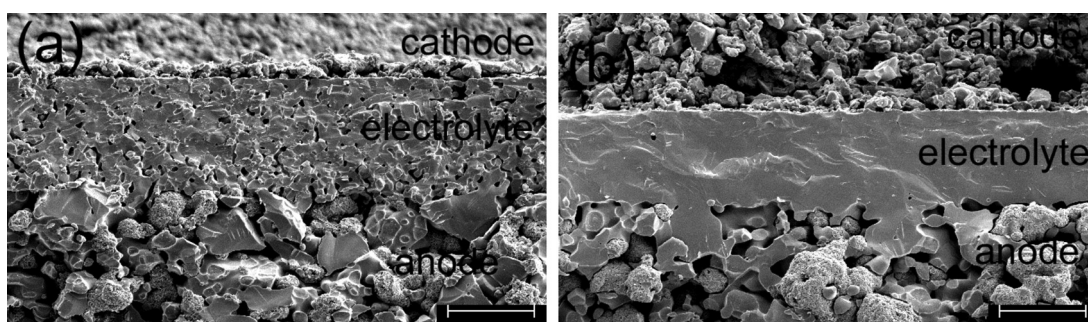


Fig. 8. SEM images of the fractured cross sections of (a) SOFC-A and (b) SOFC-B after the fuel cell tests. Micron bars show 10  $\mu\text{m}$ .

$22 \text{ mW cm}^{-2}$  at 800, 700 and 600 °C, respectively.<sup>24</sup> Recently, maximum power densities have increased to 146, 78 and  $41 \text{ mW cm}^{-2}$  at 800, 700 and 600 °C, respectively, with changing composition of NiO:MDLS in the anode substrate from 5:5 to 6:4. They are also listed in Table 2 as RE along with the impedance results. While the OCVs of the SOFC-A are similar with those of the plasma sprayed SOFC-RE, the OCVs of the SOFC-B are slightly higher than SOFC-RE though the pasted electrolyte films are much thinner than the plasma sprayed ones. This indicates that the pasted electrolyte film sintered at 1500 °C has dense structure with a smaller amount of pores and cracks running across the electrolyte film.

As for the power density, a maximum power density of the SOFC-A at 800 °C is lower than SOFC-RE, whereas that of the SOFC-B is slightly higher than RE. With decreasing temperature to 700 and 600 °C, however, power densities of the pasted electrolyte SOFC-A and B, decrease significantly compared with the SOFC-RE. The lower power densities at 700 and 600 °C are clearly attributed to higher polarization resistance of the pasted SOFCs as observed in Table 2. Note that, even at 800 °C, polarization resistance of SOFC-A and B are much higher than SOFC-RE.

Higher polarization resistance indicates lower electrode performance which includes electrode surface reaction and gas diffusion processes.<sup>25</sup> In the anode supported SOFC using the MDLS paste, the electrolyte film with the anode substrate must be sintered above densification temperature of 1400 °C. Such high sintering temperature often induces unwanted electrolyte–electrode interface reaction and sintering of fine particles in the anode substrate, which leads to reducing electrode performance.

Power densities of 112 and  $150 \text{ mW cm}^{-2}$  of the pasted electrolyte SOFCs at 800 °C seem to be low, considering thickness of the electrolyte, compared with the plasma sprayed SOFC-RE, or sintered ceramic electrolyte supported SOFCs.<sup>14–16</sup> As

mentioned above, we consider that the low power densities are mainly due to electrode microstructure and electrolyte–electrode interface reaction which were not sufficiently controlled. Relating to this, however, Jo et al. have claimed that lanthanum silicate electrolyte should be sintered above 1600 °C to have high ionic conductivity.<sup>26</sup> According to their theory, the MDLS electrolyte films of the SOFC-A and B sintered at 1400 and 1500 °C, respectively, should have low ionic conductivity and power densities. It is not favorable, however, to raise sintering temperature of the anode supported SOFCs up to 1600 °C, which may result in the serious electrolyte–electrode interface reaction and degradation in the electrode microstructure. At present, we consider 1500 °C is the best sintering temperature to fabricate dense MDLS electrolyte films from the nano-sized paste. Our next target is to realize high power density by optimizing cell structure including insertion of buffer layer<sup>16</sup> and electrode microstructure.

#### 4. Conclusions

We have successfully fabricated apatite-type MDLS films and anode supported SOFCs using nano-sized MDLS printable paste. After development of porous network structure with grain growth up to 1300 °C, densification of the paste films occurred above 1400 °C which is 200 °C lower than the conventional solid state reactions. Anode supported SOFC using the MDLS pasted film sintered at 1500 °C exhibited an OCV of 0.91 V and a maximum power density of  $150 \text{ mW cm}^{-2}$  at 800 °C which is similar with the SOFC with a thermal sprayed MDLS electrolyte film.

#### Acknowledgment

This work was supported by Adaptable and Seamless Technology Transfer Program through target-driven R&D, from Japan Science and Technology Agency (JST), Japan.

## References

1. Molenda J, Świerczek K, Zajac W. Functional materials for the IT-SOFC. *J Power Sources* 2007;**173**:657–70.
2. Brett DJL, Atkinson A, Brandon NP, Skinner SJ. Intermediate temperature solid oxide fuel cells. *Chem Soc Rev* 2008;**37**:1568–78.
3. Steele BCH. Appraisal of  $Ce_{1-y}Gd_yO_{2-y/2}$  electrolytes for IT-SOFC operation at 500 °C. *Solid State Ionics* 2000;**129**:95–110.
4. Ishihara T, Matsuda H, Takita Y. Doped  $LaGaO_3$  perovskite type oxide as a new oxide ion conductor. *J Am Chem Soc* 1994;**116**:3801–3.
5. Nakayama S, Kageyama T, Aono H, Sadaoka Y. Ionic conductivity of lanthanoid silicates,  $Ln_{10}(SiO_4)_6O_3$  ( $Ln=La, Nd, Sm, Gd, Dy, Y, Ho, Er$  and  $Yb$ ). *J Mater Chem* 1995;**5**:1801–5.
6. Tao S, Irvine JTS. Preparation and characterisation of apatite-type lanthanum silicate by a sol–gel process. *Mater Res Bull* 2001;**36**:1245–58.
7. Abram EJ, Sinclair DC, West AR. A novel enhancement of ionic conductivity in the cation-deficient apatite  $La_{9.33}(SiO_4)_6O_2$ . *J Mater Chem* 2001;**11**:1978–9.
8. Kendrick E, Islam MS, Slater PR. Developing apatites for solid oxide fuel cells: insight into structural, transport and doping properties. *J Mater Chem* 2007;**17**:3104–11.
9. Marques FMB, Kharton VV, Naumovich EN, Shaula AL, Kovalevsky AV, Yaremchenko AA. Oxygen ion conductors for fuel cells and membranes: selected developments. *Solid State Ionics* 2006;**177**:1697–703.
10. Guillot S, Beaudet-Savignat S, Lambert S, Roussel P, Vannier RN. Effect of the dopant nature on the conductivity of oxygen overstoichiometric oxyapatites with controlled microstructures. *Solid State Ionics* 2011;**185**:18–26.
11. Gasparyan H, Neophytides S, Niakolas D, Stathopoulos V, Kharlamova T, Sadykov V, et al. Synthesis and characterization of doped apatite-type lanthanum silicates for SOFC applications. *Solid State Ionics* 2011;**192**:158–62.
12. Yoshioka H. High oxide ion conductivity in Mg-doped  $La_{10}Si_6O_{27}$  with apatite-type structure. *Chem Lett* 2004;**33**:392–3.
13. Yoshioka H, Tanase S. Magnesium doped lanthanum silicate with apatite-type structure as an electrolyte for intermediate temperature solid oxide fuel cells. *Solid State Ionics* 2005;**176**:2395–8.
14. Yoshioka H, Nojiri Y, Tanase S. Ionic conductivity and fuel cell properties of apatite-type lanthanum silicates doped with Mg and containing excess oxide ions. *Solid State Ionics* 2008;**179**:2165–9.
15. Mineshige A, Nakao T, Ohnishi Y, Sakamoto R, Daiko Y, Kobune M, et al. Ionic and electronic conductivities and fuel cell performance of oxygen excess type lanthanum silicates. *J Electrochem Soc* 2010;**157**:81465–70.
16. Marrero-López D, Martín-Sedeño MC, Peña-Martínez J, Ruiz-Morales JC, Núñez P, Aranda MAG, et al. Evaluation of apatite silicates as solid oxide fuel cell electrolytes. *J Power Sources* 2010;**195**:2496–506.
17. Masubuchi Y, Higuchi M, Takeda T, Kikkawa S. Preparation of apatite-type  $La_{9.33}(SiO_4)_6O_2$  oxide ion conductor by alcoxide-hydrolysis. *J Alloys Compd* 2006:408–12, 641–4.
18. Dru S, Meillot E, Wittmann-Teneze K, Benoit R, Saboungi ML. Plasma spraying of lanthanum silicate electrolytes for intermediate temperature solid oxide fuel cells (ITSOFCs). *Surf Coat Technol* 2010;**205**:1060–4.
19. Wang WZ, Sun F, Guo XP, Liao HL, Elkedim O, Liang JC. Effect of substrate surface temperature on the microstructure and ionic conductivity of lanthanum silicate coatings deposited by plasma spraying. *Surf Coat Technol* 2011;**205**:3665–70.
20. Sun F, Zhang N, Li J, Liao H. Preparation of dense silicate electrolyte coating with low pressure plasma spraying and very low pressure plasma spraying for intermediate-temperature solid oxide fuel cells. *J Power Sources* 2013;**223**:36–41.
21. Brois P, Mazataud C, Fourcade S, Mauvy F, Grenier JC, Billard A. Synthesis and characterization of apatite structure sputter deposited coatings dedicated to intermediate temperature solid oxide fuel cells. *J Electrochem Soc* 2011;**158**:81479–84.
22. Vieira MM, Oliveira JC, Shaula AL, Cavaleiro A, Trindade B. Lanthanum silicate thin films for SOFC electrolytes synthesized by magnetron sputtering and subsequent annealing. *Surf Coat Technol* 2012;**206**:3316–22.
23. Santacruz I, Porras-Vázquez JM, Losilla ER, Aranda MAG. Preparation of aluminium lanthanum oxyapatite tapes,  $La_{10}AlSi_5O_{26.5}$ , by tape casting and reaction sintering. *J Eur Ceram Soc* 2011;**31**:1573–80.
24. Yoshioka H, Mitsui T, Mineshige A, Yazawa T. Fabrication of anode supported SOFC using plasma-sprayed films of the apatite-type lanthanum silicate as an electrolyte. *Solid State Ionics* 2010;**181**:1707–12.
25. Leonide A, Sonn V, Weber A, Ivers-Tiffée E. Evaluation and modeling of the cell resistance in anode-supported solid oxide fuel cells. *J Electrochem Soc* 2008;**155**:B36–41.
26. Jo SH, Muralidharan P, Kim DK. Raman and  $^{29}Si$  NMR spectroscopic characterization of lanthanum silicate electrolytes: emphasis on sintering temperature to enhance the oxide-ion conductivity. *Electrochim Acta* 2009;**54**:7495–501.